ACS NANO

www.acsnano.org

REVIEW

Membrane Reactors for Ammonia Production: Insights into Ammonia-Separative Membranes, Synthesis Catalysts, and Their Integration

Genevieve Yarema, Ji Yang, Akash Warty, Zixiao Liu, Liangbing Hu,* and Dongxia Liu*

Cite This: *ACS Nano* 2025, 19, 39535−39563

Read Online

ACCESS | Metrics & More | Article Recommendations | Supporting Information

ABSTRACT: Ammonia (NH_3) is one of the most widely demanded industrial chemicals, with its synthesis currently dominated by the Haber-Bosch process. Although the reaction is thermodynamically favorable at high pressures and low temperatures, it faces challenges: high pressures require costly infrastructure and energy input, while low temperatures result in slow reaction kinetics. Beyond thermodynamic considerations, high pressures are required to liquefy the NH_3 product stream, a practical necessity to separate NH_3 by condensation. Membrane reactors, which integrate chemical reaction and selective separation in a single unit, offer a promising approach to overcome these limitations by selectively removing products (e.g., NH_3) to drive the reaction forward and permit product separation at lower pressures. This review aims to advance the field of NH_3-separative membrane reactors for energy efficient and decentralized NH_3 production. Following a brief introduction to the Haber-Bosch process and membrane reactor approaches for NH_3 synthesis, the review summarizes the development history and working principles of NH_3-separative membranes and prior studies on NH_3-separative membranes and NH_3 synthesis catalysts. Drawing on the properties of membrane and catalyst materials and their operational requirements, the review then explores strategies for integrating these components into a unified NH_3-separative membrane reactor system. The goal is to inspire further research into material innovations and process optimization to advance the design and application of NH_3-separative membrane reactors for sustainable NH_3 production.

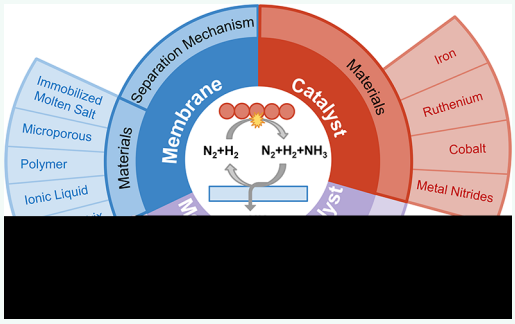

KEYWORDS: *membrane reactor, NH_3 synthesis, NH_3-separative membrane, NH_3 separation, catalysis, Haber-Bosch process, process intensification, sustainable NH_3 production*

1. INTRODUCTION

Ammonia (NH_3) is among the most widely produced chemicals globally, serving critical roles across diverse industrial sectors. Its predominant use lies in fertilizer production, which underpins global agricultural output and food security.[1] It is also a key feedstock for the synthesis of various chemicals, including dyes, cleaning agents, explosives, and plastics.[2] More recently, ammonia has gained attention as a potential energy carrier for hydrogen (H_2) transport and storage.[3] Hydrogen can be produced electrochemically from water (H_2O) using renewable electricity, offering a means of large-scale energy storage from intermittent energy sources such as solar and wind. It can subsequently be utilized without carbon dioxide (CO_2) emissions, either via combustion or conversion back into electricity through fuel cells.[4] However, the low volumetric energy density of hydrogen, along with the energy-intensive requirements for compression or liquification,[5] presents challenges for its storage and distribution. Ammonia, by contrast, is carbon-free, readily liquefied under mild conditions, and benefits from an established global infrastructure for production, storage, and transport.

The industrial synthesis of ammonia was pioneered in 1908 by Fritz Haber, who developed a method to produce ammonia from hydrogen and nitrogen (N_2) under high pressures and temperatures, incorporating a closed-loop system for unreacted

Received: July 25, 2025
Revised: October 24, 2025
Accepted: October 27, 2025
Published: November 10, 2025



ACS Publications © 2025 American Chemical Society

https://doi.org/10.1021/acsnano.5c12610
ACS Nano 2025, 19, 39535−39563

Figure 1. Effect of temperature and pressure (a), and temperature, pressure, and NH_3 separation (0−99% NH_3 removal) (b) on theoretical equilibrium N_2 conversion in the HBP. (Calculated from thermodynamic equations of the HBP (for details see Section S1 in the Supporting Information file)).

gases.[6] Carl Bosch scaled this process for industrial application, leading to the commissioning of the first commercial ammonia synthesis plant in 1911 and the establishment of the Haber-Bosch process (HBP).[7,8] Both Haber and Bosch were awarded Nobel Prizes in Chemistry in 1918 and 1931, respectively, for their foundational contributions to the modern chemical industry. Continued progress in ammonia synthesis was marked by Gerhard Ertl's Nobel Prize in 2007,[9] recognizing his elucidation of the surface chemistry of iron (Fe) catalysts central to the HBP. Today, the HBP remains the cornerstone of global NH_3 production, accounting for 500 million tons annually.

https://doi.org/10.1021/acsnano.5c12610
ACS Nano 2025, 19, 39535−39563

Table 3. Summary of Representative Fe-Based Catalysts for NH_3 Synthesis

catalyst type	reaction rate/activity	temperature & pressure	stability	ref.
Fe-based catalysts (promoted with potassium and aluminum oxide)	15−20% conversion, space velocity =10,000−30,000 h^{-1}	300−500 °C, 100−200 bar; (425 °C, 150 bar shown)	promoted with Al_2O_3 prevents sintering, stable	88−94
Fe-based catalysts (promoted with lithium hydride)	5 mmol g^{-1} h^{-1}	300 °C, 10 bar	constant catalytic activities within the testing period of 10 h	95
Fe-BaH_2 chemical looping process	1.703 ± 0.07 mmol g^{-1} h^{-1}	300 °C, 1 bar	NH_3 production rate decreased from 1.2 to 0.9 mmol NH_3 g^{-1} h^{-1} after eight cycles	96
Fe on $BaTiO_{3-x}H_x$	14 mmol g^{-1} h^{-1}	400 °C, 50 bar	not reported	97
Fe on $BaCeO_{3-x}H_yN_z$	6.8 mmol g^{-1} h^{-1}	400 °C, 9 bar	stable under optimized low-pressure conditions	98

3. AMMONIA SYNTHESIS CATALYSTS

NH_3 synthesis catalysts can be broadly categorized based on their active metal centers and structural composition. In this section, we classify the major types into four representative categories: iron-based catalysts, ruthenium-based catalysts, cobalt-based catalysts, and metal nitride catalysts. Each class has evolved with distinct mechanistic characteristics, performance profiles, and compatibility with emerging reactor designs. Figure 10 compares the activities and operating conditions of each catalyst type.

Iron-based catalysts remain the industrial standard, offering robustness and scalability under high-temperature and high-pressure conditions. Ruthenium-based systems, while more expensive, show superior intrinsic activity, especially under milder reaction environments. Cobalt-based and nitride-based catalysts have recently gained attention due to their earth abundance and unique electron-donating properties, opening new pathways for sustainable NH_3 synthesis. The following subsections summarize the structural features, synthesis strategies, reaction performance, and application prospects of each catalyst type, supported by recent experimental data. These insights not only highlight catalytic innovations but also form a basis for selecting and optimizing catalysts suitable for integration into membrane-assisted systems.

3.1. Iron-Based Catalysts. The HBP traditionally uses iron (Fe) catalysts. Iron catalyst type, reaction rate, operating conditions, and stability are summarized in Table 3. Historically, development efforts have focused on optimizing magnetite-based catalysts by modifying the Fe^{2+}/Fe^{3+} ion ratio, believed to significantly impact catalytic performance. Studies by Almquist and Crittenden[89] demonstrated that a ratio close to 0.5 optimizes activity. Although iron plays a central role, it shows negligible intrinsic activity under typical synthesis conditions, necessitating the use of promoters that enhance both the structural integrity and electronic properties of the catalysts. In the 1970s, research by Aika and Ozaki[90] on Al_2O_3 promoters showed no increase in yield, though its role in preventing sintering was confirmed. Baranski and colleagues further explored the dynamics of iron reduction in catalysts, linking reduction behaviors to variations in gas flow rate and temperature, and found that the results satisfy the Seth and Ross kinetic equation for a mixed-control mechanism in which neither the surface reaction nor the diffusion determines the reaction rate. Further explorations into the structural sensitivity of small iron particles by Dumesic[91] and the effect of potassium promoters by Van Ommen[92] highlighted the complex interplay of chemical interactions under varying conditions. Initial experiments with KOH as a promoter were detrimental under synthesis conditions due to its interaction with iron. However, subsequent studies[93] revealed that increasing the pressure could significantly enhance the catalytic activity, underscoring the potential of potassium-based promoters under optimized conditions. Additionally, iron catalysts promoted with Al_2O_3, K_2O, CaO, and SiO_2 have shown high activity,[94] achieving NH_3 conversion rates of 15−20% at 425 °C and 150 bar, with space velocities ranging from 10,000 to 30,000 h^{-1}.

Recent studies by Wang et al.[95] highlighted the significant effects of lithium hydride in enhancing the activity of iron-based catalysts, particularly when used in a 5 to 1 molar ratio relative to iron. This approach deviates from traditional methods where a larger percentage of iron is used, with only a small fraction of promoters. The resulting low-iron-content catalyst demonstrated considerable activity at significantly lower temperatures than previously observed.

Further exploration into hydride catalysts by Gao et al.[96] revealed substantial improvements in activity at reduced iron levels, particularly with a 20% Fe−BaH_2 catalyst. Their most significant findings arose from the adoption of the chemical looping process in NH_3 synthesis. This methodology involves nitridation of the hydride support under N_2 flow, which is subsequently hydrogenated to form NH_3. Utilizing this process, the activity of the 20% Fe−BaH_2 catalyst was enhanced by approximately 4.5 times and enabled NH_3 synthesis at temperatures 50 °C lower than standard conditions. The study also investigated replacing iron with nickel in the catalyst composition. Typically, nickel shows some activity toward NH_3 synthesis but not enough to outperform iron-based catalysts.[97]

Tang et al.[98] significantly advanced the development of low-iron-content catalysts by supporting iron on the oxyhydride material $BaTiO_{3-x}H_x$, achieving an impressive activity of 14 mmol g^{-1} h^{-1} at 400 °C and 50 bar with just 1 wt % iron. This high activity, despite the low iron content, was attributed to the catalyst's increased resistance to H_2 poisoning and the electron promotion effect of the oxyhydride support, which enhances the electron density at the catalytic sites. Building on this approach, Kitano et al.[99] introduced nitrogen into an oxyhydride matrix, creating a $BaCeO_{3-x}H_yN_z$ oxynitride-hydride with iron comprising 1.2 wt %. This catalyst displayed a significant activity of 6.8 mmol g^{-1} h^{-1} at 400 °C and 9 bar, highlighting the effectiveness of low iron content under optimized conditions.

3.2. Ruthenium-Based Catalysts. After multipromoted fused-iron catalysts, ruthenium-based catalysts supported on graphite carbon represent the second most utilized group for industrial NH_3 synthesis, primarily adopted in processes like the Kellogg advanced NH_3 process developed in 1980.[100] Since their initial usage in 1979, ruthenium (Ru) catalysts have attracted significant research focus, particularly in exploring various support materials that can enhance their activity. Until now, the performance of Ru-based catalysts for NH_3 synthesis

https://doi.org/10.1021/acsnano.5c12610
ACS Nano 2025, 19, 39535−39563

has been extensively studied with particular focus on the effects of support materials, Ru loading percentages, precursor forms, and impregnation methods. Ru catalyst type, reaction rate, operating conditions, and stability are summarized in Table 4. A significant advancement in understanding these catalysts was the identification of the B_5-type site as the crucial active site for Ru-based catalysts.[101] This site consists of a unique arrangement where three Ru atoms form a layer beneath a layer of two Ru atoms. The optimal Ru particle size to maximize the density of these B_5 sites is 2 nm based on geometric modeling and density functional theory calculations. This size range, specifically between 1.8 and 2.5 nm, enriches the presence of B_5 sites which facilitates the adsorption and dissociation of N_2, which are crucial steps in the synthesis of NH_3.[102] Detailed experimental studies by García-García et al.[103] have shown that particle growth, and consequently the density of B_5 sites, is influenced by the reduction temperature during catalyst preparation. Lower temperatures tend to preserve the optimal particle size and thus the activity of the catalyst. Furthermore, the addition of a barium promoter has been found to enhance the number of B_5 sites through surface reconstruction of the Ru catalyst, leading to increased catalytic activity.[104]

The research on ruthenium-based catalysts for NH_3 synthesis has demonstrated a variety of innovative approaches to enhance catalytic performance. Notably, the use of a carbon-covered Mg−Al hydrotalcite as a support material for ruthenium was introduced by Narasimharao et al. in 2016.[105] They prepared the Mg−Al hydrotalcite via a coprecipitation method and subsequently coated it with carbon through the pyrolysis of cyclohexene. The resulting supported Ru catalyst, when promoted with cesium and barium, showed an NH_3 conversion of 0.9% at ambient pressure and 327 °C. This indicates a potential pathway for utilizing hydrotalcite-based materials in NH_3 synthesis, although the conversion rates need enhancement. Further advancements in the field have been observed with the development of Ru cluster catalysts. Li et al.[106] reported that Ru/MgO-MIL with small Ru clusters of approximately 1.0 nm exhibited an NH_3 synthesis performance vastly superior to that of traditional 2−4 nm Ru/MgO catalysts. This enhanced activity was attributed to the efficient utilization of atomic clusters, which may deviate from the Wulff construction theoretical model under practical conditions and inadvertently generate more active B_5 sites.

Similar to Fe-based catalysts, Ru-based catalysts are sensitive to trace oxygenates (e.g., H_2O, O_2, CO_2), which can rapidly deactivate active sites.[107] For instance, at 350 °C and 30 bar, the NH_3 formation rate of the 5 wt % $Ru/La_{0.5}Ce_{0.5}O_{1.75}$ catalyst decreased by over 50% within 20 h when using research-grade H_2 and N_2 (>99.99%) as feed gases containing low concentrations of oxygenates like H_2O, O_2, and CO_2. Metal hydrides, amides, and oxyhydrides have proven to be outstanding support materials for Ru-based NH_3 synthesis catalysts. These materials offer protection against hydrogen poisoning and, in some cases, can shift the rate-limiting step. Notably, Ru supported on high-surface-area $12CaO{\cdot}7Al_2O_3$ electride exhibits the highest catalytic activity at ambient pressure,[108] achieving 2.290 mmol g^{-1} h^{-1} at a temperature of only 340 °C. Kobayashi et al.

Table 5. Summary of Representative Co-Based Catalysts for NH_3 Synthesis

catalyst type	reaction rate/activity	temperature & pressure	stability	ref.
Ba-promoted Co/C (carbon support treated at high temperature)	86.4 mmol g^{-1} h^{-1} nearly 2× Fe-based KM1 at same conditions	320−440 °C, 2−50 bar (440 °C, 10 bar shown)	stable activity dependent on Ba promoter, stable across varying NH_3 concentrations	118
Ba-promoted Co/C	99 mmol g^{-1} h^{-1}, TOF = 0.125 s^{-1}	400−470 °C, 90 bar	moderate activity, stable performance	119
Ba−Co_{R+P+C}/C (Ba-promoted Co with multistep treatment)	127 mmol g^{-1} h^{-1}	470 °C, 90 bar	enhanced by precise support preparation and Ba addition	120,121
Co−CeO_2 with varying surface hydroxyl properties	20 mmol g^{-1} h^{-1}	400 °C, H_2 pretreatment	promoted by surface ion optimization, stable at 430 °C for 40 h	123
Co−N−C (single-atom Co on N-doped carbon)	116.35 mmol gCo^{-1} h^{-1}	250−350 °C, 2−50 bar (350 °C, 10 bar shown)	stable for over 102 h, no aggregation of Co atoms observed	124
Co−N_2 single-atom catalysts (low Co−N coordination number (CN))	85.3 mmol gCo^{-1} h^{-1} (CN = 2) 68.8 mmol gCo^{-1} h^{-1} (CN = 3) 38.8 mmol gCo^{-1} h^{-1} (CN = 4)	300 °C, 10 bar	stable for 50 h, no aggregation of Co atoms observed	127
Ba-promoted Co_2 atomic clusters	19.42 mmol g_{cat}^{-1} h^{-1}	400 °C and 10 bar	stable for 50 h at 350 °C and 1 MPa	129

60.4 mmol g^{-1} h^{-1} at 360 °C and 9 bar. Similar to the results with BaO-CaH_2, where BaH_2 forms during catalyst pretreatment and reaction, $Ba(NH_2)_2$ is also formed, promoting the dissociative adsorption of N_2 and thereby shifting the rate-limiting step.

Hattori et al.[113] have recently demonstrated extremely low-temperature NH_3 synthesis using a Ru-based catalyst supported on a solid solution of CaFH. This catalyst achieved an activity of 0.05 mmol g^{-1} h^{-1} at ambient pressure and a near-ambient temperature of 50 °C. The CaFH support, formed from the solid solution of CaF_2 and CaH_2, benefits from weak ionic bonds between Ca^{2+} and H^-, which facilitate the release of hydrogen atoms, contributing to the catalyst's excellent performance. Also at low temperature, Wildfire et al.[114] reported microwave-assisted NH_3 synthesis using a Ru/MgO catalyst, achieving an activity of 0.613 mmol g^{-1} h^{-1} at 320 °C and ambient pressure in a 2.45 GHz microwave reactor. They found that increasing the Ru loading from 4 to 10% resulted in a lower metal site temperature and quicker response time, highlighting the significant impact of Ru loading on this synthesis method. Although the activity was not as high as the best-performing Ru catalysts under conventional conditions, this study opens the door for applying microwave-assisted synthesis to other higher-activity Ru-based catalysts.

Despite the high activity of Ru-based catalysts at reduced temperatures and pressures, the global production of ruthenium in 2017 was only 35.5 tonnes.[115] If an NH_3 synthesis plant requires 300 tonnes of catalyst with 2 wt % Ru, this would consume approximately 6 tonnes of Ru, which is about 17% of the annual global production. This significant demand would sharply increase Ru prices, explaining why only about ten NH_3 synthesis plants worldwide use Ru-based catalysts. The majority of the market remains dominated by cheaper fused-iron-based catalysts. Wang et al.[116] employed HZSM-5 zeolite, with its rich microporous structure, as an anchoring site to stabilize Ru single atoms (Ru/HZ SAC) using a microwave single-mode and ion-exchange method. The Ru/HZ SAC with 0.2 wt % Ru exhibited an NH_3 synthesis rate of 4.67 mmol NH_3 g^{-1} h^{-1} at 350 °C and 10 bar, approximately 20 times higher than Ru/HZ nanoclusters. Additionally, the apparent activation energy for NH_3 synthesis over Ru/HZ SAC (38 kJ mol^{-1}) was significantly lower than that of conventional Ru-based catalysts (80−130 kJ mol^{-1}), indicating a different reaction mechanism.[117]

3.3. Cobalt-Based Catalysts. In recent years, cobalt-based NH_3 synthesis catalysts have garnered significant attention due to their high activity. Similar to ruthenium, cobalt-based catalysts typically use support materials, which can be incorporated in varying weight percentages, ranging from small amounts as seen in multipromoted fused-iron catalysts to higher amounts similar to those used for Ru-based catalysts. Cobalt (Co) catalyst type, reaction rate, operating conditions, and stability are summarized in Table 5.

In 2002, Hagen et al.[118] explored the catalytic activity of a barium-promoted Co catalyst supported on carbon for NH_3 synthesis. The catalytic activity was assessed over a temperature range of 320−440 °C and a pressure range of 2−50 bar. They found the highest activity at 440 °C and 10 bar with a H_2/N_2 mole ratio of 3:1, achieving a rate of 86.4 mmol g^{-1} h^{-1}. In 2006, Raróg-Pilecka et al.[119] investigated how the preparation method affected the catalytic activity of carbon-supported Co catalysts for NH_3 synthesis. The catalytic activity of these catalysts was measured at 90 bar with a H_2/N_2 mole ratio of 3:1 over a temperature range of 400−470 °C. The highest activity was observed at 470 °C using the Ba−Co_{R+P+C}/C catalyst, with a rate of 127 mmol NH_3 g^{-1} h^{-1}. In 2007, Raróg-Pilecka et al.[120] further examined the treatment methods for the carbon support used in Co catalysts. When evaluated at 90 bar, 400 °C, with a stoichiometric H_2/N_2 gas flow, the highest activity was observed for the catalyst supported on the treated GF_{45} support, with a rate of 89 mmol NH_3 g^{-1} h^{-1}. In 2008, Raróg-Pilecka et al.[121] revisited the use of Co as an NH_3 synthesis catalyst by employing activated carbon as a template to create an unsupported Co catalyst. The doubly promoted catalyst, featuring both cerium and barium, showed the highest activity, achieving 116 mmol NH_3 g^{-1} h^{-1} at 63 bar and 400 °C with a H_2/N_2 ratio of 3:1. In 2011, Raróg-Pilecka et al.[122] further investigated the preparation of doubly promoted Co catalysts using the coprecipitation method. Catalyst activity was tested at 6.2 MPa with a H_2/N_2 ratio of 3:1, and the doubly promoted catalyst again showed the highest activity, with a turnover frequency of 0.370 s^{-1} at 430 °C.

In 2014, Lin et al.[123] developed a Co catalyst supported on ceria for NH_3 synthesis. They created a series of Co/CeO_2 catalysts with varying surface hydroxyl group properties by altering the pretreatment method. High catalytic activity was noted for catalysts reduced in H_2 at high temperatures, likely due to the formation of surface hydroxyl ions that react with

https://doi.org/10.1021/acsnano.5c12610
ACS Nano 2025, 19, 39535−39563

Table 6. Summary of Representative Metal Nitride Catalysts for NH_3 Synthesis

catalyst type	reaction rate/activity	temperature & pressure	stability	ref.
Co_3Mo_3N	0.986 mmol h^{-1} g^{-1} (with Cs promotion, Cs/Co = 0.02)	400 °C, 1 bar	improved with Cs/K promoters	132,133
$K_2[Mn(NH_2)_4]$	11 mmol g^{-1} h^{-1}	400 °C, 10 bar	high activity at lower pressures	135
$Rb_2[Mn(NH_2)_4]$	6 mmol g^{-1} h^{-1}	400 °C, 10 bar	higher activity than traditional nitrides	135
Ni−CeN	6.5 mmol g^{-1} h^{-1}, WHSV = 36,000 mL g^{-1} h^{-1}	400 °C, 9 bar	nitrogen vacancies enhance N_2 activation	136,137
Co/SrNH	1686.7 mmol gCo^{-1} h^{-1}, TOF > 500 h^{-1}	400 °C, 9 bar	stable for 100 h, robust against NH_3 inhibition	138

H_2 to form water, thus freeing the active sites for N_2 absorption. In 2015, Tarka et al.[124] studied the impact of barium promotion on the stability and activity of carbon-supported Co catalysts for NH_3 synthesis. Catalysts with 27.4 wt % Co and varying barium promoter content (0 to 0.88 mmol g^{-1} C + Co) were tested at 90 bar, 400 °C, with a H_2/N_2 ratio of 3:1. The optimal barium content was found to be 0.68 mmol g^{-1} (C + Co), achieving an NH_3 synthesis rate of 88 mmol gC + Co^{1-} h^{-1}.

The development of non-noble metal single-atom catalysts (SACs) has garnered significant interest for industrial applications due to their cost-effectiveness and high activity. Carbon materials and N-doped carbon materials are particularly promising supports for SACs, offering large specific surface areas, adjustable electronic structures, and efficient electron transfer capabilities.[125] In this regard, Wang et al.[126] demonstrated the efficacy of N-doped carbon-supported Co SACs (Co−N−C) for NH_3 synthesis under mild conditions. At 350 °C and 10 bar, the Co−N−C catalyst achieved an NH_3 synthesis rate of 4.34 mmol g_cat^{-1} h^{-1}, which was 11- and 17-fold higher than that of Co/C and N−C, respectively. This exceptional performance is attributed to the synergistic effect of dynamic and steady-state dual-active sites. The stable Co_1−$N_{3.5}$ active site, formed by the coordination of Co with pyrrolic N in the support, facilitates N_2 activation via an associative mechanism, leading to stepwise hydrogenation and the eventual release of NH_3. Additionally, pyridine N species, interacting less strongly with Co, can react with adsorbed H_2 to form NH_3 via a chemical looping pathway.

Zhou et al.[127] explored the impact of different coordination environments in SACs on NH_3 synthesis performance by preparing atomically dispersed Co-based catalysts with varying Co−N coordination numbers through different pyrolysis temperatures. As the pyrolysis temperature increased, the Co−N coordination number decreased. SACs with Co−N_4, Co−N_3, and Co−N_2 coordination structures were obtained at 450, 550, and 650 °C, respectively. The Co−N_2 catalyst, with the lowest coordination number, exhibited the highest catalytic activity, achieving an NH_3 synthesis rate of 85.3 mmol NH_3 gCo^{1-} h^{-1} at 300 °C and 10 bar. Li et al.[128] also studied Co SACs with varying Co−N coordination numbers, confirming that Co−N_2 catalysts with two coordination N atoms showed the best NH_3 synthesis performance due to improved N_2 adsorption and activation. Further research by Peng et al.[129] focused on NH_3 synthesis using nonprecious metal cluster catalysts. They synthesized cobalt atomic dimers on a nitrogen−carbon support (Co_2 ACCs) and compared them with Co SAC and Ru nanoparticles references. At 400 °C and 10 bar, Co_2 ACCs achieved a high NH_3 synthesis rate of 8.54 mmol NH_3 g_cat^{-1} h^{-1}, approximately 1.8- and 3.3-fold higher than Co SAC (4.60 mmol g_cat^{-1} h^{-1}) and Co nanoparticles (2.55 mmol g_cat^{-1} h^{-1}), respectively.

3.4. Metal Nitride Catalysts. The exploration of metal nitride catalysts in NH_3 synthesis has evolved to include both binary and more complex ternary systems, demonstrating significant advancements in catalytic performance. These developments highlight a strategic move away from traditional noble metal catalysts to more robust and potentially more efficient nitride-based systems. The utilization of binary nitrides involving metals like uranium, cerium, vanadium, molybdenum, and rhenium has been well documented,[130] with historical reports dating back to the early works of Haber who explored the catalytic capabilities of uranium nitrate. However, the transformative development in this field has been the conceptualization and realization of ternary nitride systems. These catalysts blend the properties of two different metals to optimize N_2 adsorption energies, thereby enhancing NH_3 synthesis rates.[131] Iron catalyst type, reaction rate, operating conditions, and stability are summarized in Table 6.

Combining two metals to create a ternary nitride system, where one metal has a high N_2 adsorption energy and the other has a low N_2 adsorption energy, can result in an NH_3 synthesis catalyst with a turnover frequency closer to the optimal level than any single metal nitride. For instance, in the Co−Mo catalyst system, molybdenum binds N_2 too strongly, while cobalt binds N_2 too weakly. This concept was experimentally validated by Jacobsen,[132] who tested ternary nitride catalysts such as Fe_3Mo_3N, Co_3Mo_3N, and Ni_2Mo_3N with promoters. In 2001, Kojima and Aika[133] investigated the preparation method for Co_3Mo_3N catalysts and its impact on NH_3 synthesis activity. The catalyst's activity was tested at 400 °C and 1 bar with a gas flow rate of 45 mL min^{-1} H_2 and 15 mL min^{-1} N_2. The unpromoted Co_3Mo_3N catalyst achieved a rate of 0.652 mmol h^{-1} g^{-1}, which increased to 0.869 mmol h^{-1} g^{-1} with potassium promotion (K/Co mole ratio of 0.05). The highest rate, 0.986 mmol h^{-1} g^{-1}, was achieved with cesium promotion (Cs/Co mole ratio of 0.02). Azofra et al.[134] developed single molybdenum active sites within Si-based materials for NH_3 synthesis. At 400 °C and atmospheric pressure, the NH_3 synthesis rate was 1.3 mmol gMo^{-1} h^{-1}. Theoretical studies suggested that N_2 spontaneously adsorbed and activated on the [(Si−O−)MoH_3] site via an associative mechanism, with the rate-determining step being the further hydrogenation of the adsorbed *$NHNH_2$ to form NH_3. Cao et al.[135] expanded on the concept of ternary nitrides by investigating ternary amides of transition and alkali metals. They synthesized $Rb_2[Mn(NH_2)_4]$ and $K_2[Mn(NH_2)_4]$ through ball milling the respective metals at room temperature under 7 bar of NH_3. Both exhibited significantly higher activities compared to the best performing ternary nitride catalyst, Co_3Mo_3N. Specifically, $K_2[Mn(NH_2)_4]$ showed an activity of 11 mmol g^{-1} h^{-1}, $Rb_2[Mn(NH_2)_4]$ had 6 mmol g^{-1} h^{-1}, and Co_3Mo_3N achieved 5.3 mmol g^{-1} h^{-1}. One of the significant challenges in NH_3 synthesis is achieving high activity at low temperatures.[136] The study by Ye et al.[137] on the

https://doi.org/10.1021/acsnano.5c12610
ACS Nano 2025, 19, 39535−39563

Ni−CeN catalyst system has provided critical insights into the dynamic processes of NH_3 synthesis via novel catalyst designs. Achieving an impressive activity of 6.5 mmol g^{-1} h^{-1} at conditions of 400 °C, 9 bar, and a WHSV of 36,000 mL g^{-1} h^{-1}, the system underscores the significant role of nitrogen vacancies within the CeN matrix for effective N_2 activation, coupled with Ni's capability for H_2 activation. This innovative approach transforms traditional catalyst and promoter roles into a cohesive cocatalyst framework, where each component specifically addresses distinct aspects of the NH_3 synthesis process. In this setup, Ni's strong affinity for H_2 (−1.30 eV) contrasts with the relatively milder affinity for nitrogen vacancies (−0.62 eV) within CeN, steering the H_2 adsorption and dissociation primarily toward the Ni sites. This specificity facilitates the preferential formation of NH_3 via interactions between adsorbed H_2 and lattice nitrogen from CeN, enhancing the catalyst's efficiency. Traditional scaling relations pose challenges, but recent work by Ye and co-workers[138] demonstrated that alkali earth imides (AeNH) combined with transition metals (e.g., Fe, Co, and Ni) can overcome these limitations. This combination leverages active defects on the support surface and the loaded transition metals, enabling multiple reaction pathways for NH_3 production. For example, Co/SrNH exhibited a reaction rate of 1686.7 mmol gCo^{-1} h^{-1} and TOFs above 500 h^{-1} at 400 °C and 9 bar, surpassing other Co-based catalysts and even the benchmark Cs−Ru/MgO and industrial wüstite-based Fe catalysts under the same conditions.

Recent breakthroughs in NH_3 synthesis have increasingly centered on the development of high-performance catalysts capable of operating under mild conditions with high activity and selectivity. A notable contribution comes from Ye and co-workers,[138,139] whose pioneering work has consistently pushed the frontier in catalyst design through the integration of advanced nanostructures and interface engineering strategies. In particular, their atomically dispersed Ru catalysts supported on oxygen-deficient perovskites or hydride-based supports exhibit exceptional turnover frequencies, outperforming many conventional systems under comparable conditions. These systems exploit strong metal−support interactions and tailored electronic structures to enhance N_2 activation and hydrogenation kinetics. Moreover, Ye's team has explored dynamic catalytic processes such as chemical looping and nonthermal plasma-assisted synthesis,[140] achieving unprecedented reaction rates while simultaneously addressing challenges of energy efficiency and catalyst regeneration. Across their work, a unifying theme lies in the rational design of reaction interfaces whether via oxygen vacancies, imide-hydride ensembles, or electrochemical environments which significantly modulate activation barriers and mechanistic pathways. Similarly, studies of electrocatalytic and photocatalytic systems[141] reveal that while tailored defects and quantum confinement enhance N_2 activation, the operational durability of these materials remains a bottleneck due to their poor tolerance to environmental perturbations. Addressing these issues requires not only the development of robust catalyst supports and protective interfaces but also improved reactor and purification strategies to control gas-phase purity and long-term catalyst viability. Future research should place greater emphasis on catalyst stability and scalability under realistic process conditions, which remains underexplored despite substantial progress in activity and selectivity metrics. Together, these innovations mark a major step toward sustainable and scalable NH_3 synthesis beyond the traditional Haber-Bosch framework.

4. AMMONIA-SEPARATIVE MEMBRANE REACTORS

The traditional HBP relies on a cryogenic condenser to recover the synthesized NH_3, which contributes to high capital and production costs (Figure 11a). Replacing condensers with membrane separators for NH_3 separation and recovery could reduce energy consumption and lower production costs, since a membrane would operate at ambient or elevated temperatures and would require much less energy to cool and reheat the recycle stream compared to cryogenic condensation (Figure 11b). Membrane reactors, which combine reaction and separation in a single unit, offer a promising route for process intensification. They are particularly well-suited for efficient, decentralized NH_3 production at small scales (Figure 11c). However, their implementation in the HBP requires the integration of both catalyst and membrane, with careful alignment of operating temperature and pressure to ensure optimal performance. This integration presents significant technical challenges, and as a result, few studies have explored the potential of these intensified membrane reactor systems.

Figure 11. Schematic illustration of traditional HBP (a), recycle membrane reactor (b), and catalytic membrane reactor (c).

In the context of integrating NH_3 synthesis catalysts with membrane reactor systems, catalyst selection and dispersion strategies play a pivotal role in ensuring long-term stability and efficiency. Catalysts intended for use in membrane reactors

https://doi.org/10.1021/acsnano.5c12610
ACS Nano 2025, 19, 39535−39563

Figure 12. Schematic illustrations of catalytic membrane reactor configurations modeled by Wolden and co-workers[3] (a) and Gallucci and co-workers.[24] (Adapted with permission under a Creative Commons CC BY 4.0 license from ref 24. Copyright 2024 Elsevier.) (b).

must possess not only high intrinsic activity but also robust thermal and chemical compatibility with the membrane material. Ruthenium- and cobalt-based catalysts supported on stable oxides such as MgO, Al_2O_3, or CeO_2 are promising candidates due to their strong metal−support interactions, which help suppress particle agglomeration and maintain dispersion under elevated temperatures. Additionally, hydride-based supports (e.g., BaH_2, CaH_2), as discussed in recent literature, offer enhanced electron-donating ability but must be handled with care due to their sensitivity to oxygen and moisture.

Regarding catalyst incorporation, conventional techniques such as wet impregnation and sol−gel methods can be adapted to disperse active metal species within porous ceramic membranes. More advanced methods, including electrospinning and atomic layer deposition (ALD), offer better control over nanoparticle size and uniformity, which is critical for minimizing diffusion resistance and maximizing active surface area within membrane pores. Moreover, the development of catalytically active composite membranes, where catalytic nanoparticles are embedded within the matrix of proton- or electron-conductive polymers (e.g., Nafion, PBI), is a growing area of interest. Further research is needed to optimize the interface compatibility and to mitigate issues such as catalyst leaching or pore blockage during long-term operation. Overall, identifying membrane-compatible catalysts with stable dispersion behavior remains a key challenge and opportunity for advancing membrane-assisted NH_3 synthesis.

4.1. Recycle Membrane Reactor for Ammonia Synthesis. A step toward development of NH_3-separative membrane reactors is the design of a recycle membrane reactor (RMR), a concept that has motivated research into NH_3-permeable membranes for downstream separation in syngas loops in the past decades. The feasibility of this concept was first explored by Tsuru and co-workers in 2024.[28] In their study, the RMR consists of a catalytic reactor coupled in series with a membrane separator, where the retentate stream is recycled back to the reactor, as illustrated in Figure 11b. A Ru (10 wt %)/Cs/MgO catalyst was packed in the catalytic reactor and two types of membranes with different permeation properties and NH_3 selectivity were used for separation: Aquivion/ceramic composite and sulfonated (3-mercaptopropyl)trimethoxysilane (MPTMS). By independently controlling the temperature of the reactor and membrane separator, the NH_3 mole fraction in the permeate stream was significantly increased from 0.01 (at equilibrium) to 0.1−0.45 across the system, surpassing the equilibrium reaction at 350 °C. Due to the different operating temperatures between the reactor and separator, heat management plays a crucial role in influencing the performance of the RMR. A one-dimensional, isothermal, and plug-flow model was proposed to mathematically simulate the RMR, providing insights into its behavior. Although the RMR, with separate units for catalytic reaction and membrane separation, does not shift the equilibrium in the same way as a catalytic membrane reactor (where reaction and separation occur in one unit), the recycle reaction can enhance overall reaction conversion. This makes it an effective method when reaction and separation conditions are limited.

4.2. Ammonia-Separative Catalytic Membrane Reactor. The NH_3-separation membrane reactor has been studied primarily by modeling in the past few years. One study by Wolden and co-workers[3] modeled a standard industrial iron catalyst integrated with an inorganic NH_3-separative membrane in a catalytic membrane reactor. The reactor comprises an NH_3-separative membrane deposited on the exterior of a tubular support with bulk iron catalyst packed in the lumen (Figure 12a). The reactor is assumed to operate at steady state, and at isothermal and isobaric conditions. They found that conversion and NH_3 recovery are dictated primarily by the NH_3 permeance. The membrane must have a minimum permeance of 100 GPU for benefits to be significant. The NH_3 selectivity over N_2 and H_2 must each be at least 10 for the membrane to have a significant effect on conversion and NH_3 purity scales with the effective selectivity. Increasing the operating pressure significantly improves both the reaction and separation performance, and NH_3 is nearly completely recovered at 30 bar, enabling the direct recycling of unreacted H_2 and N_2 without the need for recompression. The reaction conversion increases with temperature, but the temperature can be reduced to as low as 300 °C while achieving conversion

https://doi.org/10.1021/acsnano.5c12610
ACS Nano 2025, 19, 39535−39563

levels surpassing equilibrium limits at 400 °C in a conventional reactor.

Another modeling study was done by the Gallucci group,[24] where they integrated a ruthenium catalyst in a catalytic membrane reactor (CMR) with inorganic membranes that are selective to NH_3 over N_2 and H_2. Opposite to the Wolden et al. reactor model design, the reactor in the study is structured with an inner membrane tube and an outer shell hosting the catalyst. A multitubular fixed bed membrane reactor is analyzed by scaling from a single tube to multiple tubes (Figure 12b). To enhance NH_3 transfer, the study explores using a pressure gradient or a sweep gas of similar composition as the feed, which can be applied separately or together. The study develops a simplified steady-state membrane model using a one-dimensional plug flow reactor approach. It includes mass and energy balances, the Ergun equation for pressure drop predictions, and assumes a unitary catalyst effectiveness factor, implying no internal diffusion limitations. The CMR model was integrated into several Power-to-Ammonia (PtA) process layouts, which were optimized and techno-economically compared against a traditional PEM-based PtA production process that uses condensation for separation. They found that the membrane reactor was able to achieve over 90% higher NH_3 conversion compared to conventional reactors. The conversion and recovery were enhanced independent of selectivity in processes with a sweep gas as long as the NH_3/H_2 selectivity was greater than 10−20. However, highly selective membranes are needed to produce pure NH_3 permeate, which is difficult to achieve with current membrane technology. Optimizing the energy efficiency for each process layout revealed that incorporating a membrane reactor increased the system efficiency by about 8% compared to traditional PtA processes, and the efficiency was increased by nearly double that when using solid oxide electrolysis to produce H_2 instead of PEM. However, the membrane reactor showed a 2% increase in cost compared to the reference process and a 10% increase in cost when also incorporating solid oxide electrolysis.

Since many membrane materials operate below catalyst activation temperatures to maintain stability or otherwise lose selectivity at higher temperatures, heat management in integrated membrane reactors is important. A modeling study by Kucuk et al.[25] reported on a microstructured membrane reactor that integrates reaction, cooling, and NH_3 separation functions within a single unit. The reactor model is based on data from a bulk iron catalyst and a $ZnCl_2$ IMS membrane on a zirconia support, with integrated reaction and permeate microchannels, shown in Figure 13. The proposed microchannel reactor design enables heat transfer between the neighboring reaction and permeate channels, taking the exothermic nature of the reaction into account. The model is used to understand the effects of inlet temperature, pressure, composition, space velocity, and relative flow rates of the reactive and sweep streams on the performance and operability of the reactor. When operating at inlet conditions of 340 °C, 50 bar, $H_2/N_2 = 3$, space velocity of 1.5×10^3 m^3 kg_{cat}^{-1} s^{-1}, and molar inlet sweep-to-reactive mixture flow ratio of 50, the membrane reactor achieves 47% N_2 conversion, which exceeds the thermodynamic limit. Without the membrane, N_2 conversion is only 13.5%, therefore the membrane theoretically improves conversion by about 350%. Feed temperature and pressure positively affect N_2 conversion, total NH_3 production, and NH_3 recovery in the permeate. Increasing the temperature of both the reaction and permeate inlet channels by 30 °C results in a 39% improvement in NH_3 recovery, while increasing the pressure of both the reaction and permeate inlet channels from 30 to 50 bar results in approximately 100% improvement. Lower H_2/N_2 ratios result in higher N_2 conversion and NH_3 production, as a H_2/N_2 ratio of 2 resulted in N_2 conversions as high as 1.8 times the thermodynamic limit, while the opposite trend is observed with a H_2/N_2 ratio of 4. Increasing the space velocity from 1.5 to 3×10^3 m^3 kg_{cat}^{-1} s^{-1} decreased N_2 conversion by 29%. Reducing space velocity by elongating contact of the reactive mixture with both the catalyst and membrane is favorable as long as the exothermic temperature rise can be kept below the membrane operating limit with integrated cooling, where the minimum sweep-to-reactive mixture flow ratio is 50 to meet this condition. The reactor without the membrane is not nearly as sensitive to changes in inlet temperature, inlet pressure, H_2/N_2 ratio, or space velocity.

Tsuru and co-workers

4.3. Future Development for Ammonia-Separative Membrane Reactors. *4.3.1. Membrane Reactor Operating at HBP Conditions.* NH_3 synthesis in the HBP is typically conducted at temperatures of 400−500 °C and pressures of 100−300 bar, using iron-based catalysts. It is challenging to employ a catalytic membrane reactor at HBP conditions due to the lack of membranes that are thermally stable coupled with the need for high-performance membrane materials under these conditions. Therefore, membrane materials development should be a main focus for these application conditions. Among organic, molten salt, microporous, and mixed-matrix membrane materials, microporous membranes, particularly zeolites, show the most promise due to their thermal and chemical stability. Achieving high NH_3 permeability and selectivity from the syngas mixture (e.g., H_2 and N_2) should be improved. In microporous membranes, both permeance and selectivity increase with feed pressure, which is favorable for NH_3 synthesis reactor conditions. However, NH_3 uptake by microporous adsorbents decreases with rising temperature, leading to reduced selectivity. Further development is needed to optimize the separation performance of zeolite membranes at higher temperatures. This type of membrane material can be advanced for the HBP by precisely designing the pore size and controlling NH_3 adsorption, which can be done for zeolites by adjusting the Si/Al ratio or ion-exchanging. NH_3 adsorption has been controlled in other porous materials by incorporating sodium ions[2] or sulfonic acid groups[69,70] in the nanochannel.

Molten salt membranes are another potential membrane material for HBP operations. The reported IMS, however, have not been implemented under HBP conditions due to the chemical and physical stability of the tested materials. Other molten salts could be used to optimize the IMS membrane performance. Metal halide salts, particularly molten chloride salt mixtures, have shown higher melting points and their operation window is compatible with HBP conditions.[62] However, the selective carrier-assisted diffusion mechanism in IMS membranes is only dominant at low pressures, with the less selective ordinary diffusion becoming more dominant at higher pressures. Therefore, if these membranes are integrated into a membrane reactor, the reactor would need to operate at lower pressures for the membrane to remain selectively permeable. Once the molten salt materials are determined, the design of the membrane support must be considered, as the stability of the IMS membrane is important under HBP conditions. The IMS system consists of coexisting gas, liquid, and solid that requires interfacial design to ensure that the molten salt has enough fluidity for easy diffusion, but enough cohesion and adhesion to the support to not dry out or evaporate. The pore size, thickness, and hydrophobicity of the support play a major role in the stability of the membrane, but this has not been thoroughly investigated experimentally or by modeling. IMS membranes should be paired with catalysts that operate with high activity near ambient pressures, such as Ru/CaH_2 with a BaO promoter, Ru SACs, and Co SACs, depending on the operating temperature required by the salt. The individual chemical compatibility of the salt and catalyst should also be considered, since metal halides are common choices for NH_3 separation, but some catalysts are deactivated by chloride and would be incompatible with those salts. Though IMS membranes are promising for NH_3 synthesis membrane reactors, more investigation is needed on the interaction between the molten salt and the membrane support at the target temperatures to optimize membrane stability.

4.3.2. Membrane Reactor Operating at Mild Conditions. By overcoming thermodynamic limitations, the membrane reactor has the potential to shift NH_3 synthesis from the HBP to milder conditions, such as lower pressures and temperatures, thus reducing both capital and operational costs. It also enables economically feasible decentralized NH_3 production. However, a key challenge is developing a catalyst that can activate N_2 at lower temperature conditions. Ru-based catalysts are more efficient for processes at lower pressures and temperatures, with the lowest reported temperature at 50 °C. Therefore, further development of Ru-based catalysts is needed to optimize NH_3 membrane reactors for mild reaction conditions. Despite the relatively limited number of studies, current research efforts are focused on reducing reaction temperatures to establish a benchmark for mild conditions in NH_3 synthesis. Most catalyst activity studies are conducted under pressures of less than 30 bar, which is typical for laboratory-scale experiments. However, to demonstrate the catalyst's resilience to hydrogen poisoning, it is necessary to evaluate its activity at higher pressures, a factor that many reports overlook. The higher material cost of Ru catalysts is another factor hindering their widespread use. As a result, future research should aim to improve the dispersion of Ru nanoparticles in highly mesoporous and microporous supports.

In terms of membrane materials for milder conditions, polymer and mixed-matrix membranes are promising due to their ease of processability. Polymer membranes can achieve high theoretical selectivities and they can withstand the elevated pressures favored by the NH_3 synthesis reaction. For example, Nafion membranes are stable up to 240 °C and maintain a NH_3/N_2 selectivity of 60 at 200 °C, which is enough to have a positive effect on conversion according to the modeling studies. However, Nafion membranes lose selectivity in mixed gas systems, so further development is needed to maintain selectivity under reactor conditions, most likely by cross-linking the polymer. Sulfonated block copolymers have a better separation performance under reactor gas compositions, and commercial Aquivion membranes on ceramic composite supports have been shown to maintain good selectivity at 200 °C. More work is needed to improve separation performance and membrane stability at higher temperatures if other polymeric membranes are to be used within the NH_3 synthesis reactor. Integrating porous materials such as MWCNTs in the polymer matrix can improve thermal stability and permeance, but this may further decrease selectivity. Integrating MOFs or transition metals in the polymer matrix can improve NH_3 affinity, which would improve selectivity.

4.3.3. Decoupling Catalytic Reactor and Membrane Separator. An immediate promising pathway toward the development of catalytic membrane reactors could involve operating the catalyst and membrane under different temperature and/or pressure conditions to compensate for the disadvantages of current available catalysts and membrane materials developed for NH_3 synthesis. This can be achieved spatially and/or temporarily. For example, Tsuru and coworkers[28] investigates membrane separation and catalytic reactors in series, demonstrating overall NH_3 conversion higher than the catalytic reactor alone. The challenge lies in heat integration to maintain flow operation of catalytic reactor and membrane separator at different conditions.

Another option is integrating the catalytic reactor and membrane separator into a single unit but operating them under different conditions. This could involve electrified

https://doi.org/10.1021/acsnano.5c12610
ACS Nano 2025, 19, 39535−39563

heating, which has been actively pursued in recent years for the decarbonization of process heating.[142] A feature of this heating method is the heating nonuniformity. The reactor could be designed to utilize electrified heating to create localized heating zones that would allow the catalyst to operate at higher temperatures while the membrane operates below catalyst activation temperature to maintain stability. Microwave, joule heating, and plasma would be suitable for these applications. However, the design of the heating pattern and the integration of these heating elements with the membrane and reactor components present significant challenges. Nonthermal plasma produces high-energy electrons that excite the ground state gas molecules to participate and react effectively on selective surfaces at lower temperature and atmospheric pressure,[143] although direct contact with the plasma could also decompose the membrane. Microwave heating requires dielectric materials to directly transmit electromagnetic energy to thermal energy, so the catalyst or catalyst support must include these materials to act as heating elements while the membrane does not in order to create localized heating zones. Joule heating produces heat by flowing an electric current through a conductive material. This method would require a conductive and continuous heating element throughout the reactor that has good contact with the catalyst but maintains some distance from the membrane. For both microwave and joule heating methods, the distance of the membrane from the heating element would dictate the temperature difference between the catalyst and membrane. A larger temperature difference would enable the use of a wider range of membrane materials and a wider array of membrane and catalyst combinations.

Temporal control of the heating patterns (or energy inputs) can also be applied. Electrified heating methods have much faster response times than conventional heating methods due to reduced intrinsic heat transfer limitations. This allows the heat to be rapidly pulsed and quenched, which can be used to further control the temperature difference between catalytic reactor and membrane separator. The work by Hu and coworkers[144] showed that a high peak temperature of 1127 °C can be achieved to activate N_2 and a lower reactor wall temperature around 327 °C was attainable to minimize secondary reactions. Coordinating the pulsing rate with the time scale needed to break the N_2 triple bond and the quenching rate with the time scale for N_2 adsorption on the catalyst would further optimize the reactor performance. As long as the membrane is not in direct contact with the heating element, it would only experience the average temperature of the reactor, which would be much lower than the peak pulse temperature.

5. CONCLUSIONS AND PROSPECTS

Conceptually, NH_3-separative membrane reactors offer a promising strategy for enhancing the energy efficiency of NH_3 synthesis. By leveraging Le Châtelier's principle to shift the reaction equilibrium, these systems enable higher conversions under milder operating conditions. However, practical implementation remains limited, with only a few studies reported to date. The key challenges lie in the lack of NH_3-separative membrane materials that can withstand the high-temperature, high-pressure conditions required by well-established catalysts used in the Haber-Bosch process. Conversely, there is also a limited availability of catalysts that perform effectively at the lower temperatures compatible with currently available NH_3-separative membranes, such as polymer-based materials.

This review provides a comprehensive comparison of membrane materials for NH_3 separation, detailing their separation mechanisms, operating conditions, and performance metrics. It also includes a brief overview of catalyst materials studied for NH_3 synthesis, summarizing their working conditions and catalytic performance. Based on this analysis, the review offers several recommendations for advancing NH_3-separative membrane reactor technologies: (1) the development of new membrane materials compatible with state-of-the-art HBP catalysts under HBP conditions; (2) the design of catalysts tailored for use with existing NH_3-separative membranes, particularly polymer-based systems; and (3) the integration of innovative process and reactor engineering strategies, such as spatially and temporally localized electrified heating, to decouple the operating conditions of membranes and catalysts, thereby enabling more flexible and efficient reactor designs. It is anticipated that this review will stimulate further research and innovation in membrane reactor technologies for NH_3 synthesis, with the potential to intensify the process by improving energy efficiency and enabling flexible, modular, decentralized deployment.

ASSOCIATED CONTENT

Supporting Information

The Supporting Information is available free of charge at https://pubs.acs.org/doi/10.1021/acsnano.5c12610.

Thermodynamic equations used to plot Figure 1 and tables of the separation performance, operating conditions, and membrane geometries of the membranes in Figure 4 (PDF)

AUTHOR INFORMATION

Corresponding Authors

Liangbing Hu – *Department of Electrical and Computer Engineering, Yale University, New Haven, Connecticut 06511, United States;* orcid.org/0000-0002-9456-9315; Phone: (+1) 203-737-4996; Email: liangbing.hu@yale.edu

Dongxia Liu – *Department of Chemical and Biomolecular Engineering, University of Delaware, Newark, Delaware 19716, United States;* orcid.org/0000-0001-8712-2219; Phone: (+1) 302-831-6725; Email: liud@udel.edu

Authors

Genevieve Yarema – *Department of Chemical and Biomolecular Engineering, University of Delaware, Newark, Delaware 19716, United States*

Ji Yang – *Department of Electrical and Computer Engineering, Yale University, New Haven, Connecticut 06511, United States*

Akash Warty – *Department of Chemical and Biomolecular Engineering, University of Delaware, Newark, Delaware 19716, United States;* orcid.org/0009-0008-1372-2586

Zixiao Liu – *Department of Chemical and Biomolecular Engineering, University of Delaware, Newark, Delaware 19716, United States*

Complete contact information is available at: https://pubs.acs.org/10.1021/acsnano.5c12610

Notes

The authors declare no competing financial interest.

https://doi.org/10.1021/acsnano.5c12610
ACS Nano 2025, 19, 39535−39563

ACKNOWLEDGMENTS

This material is based upon work supported by the U.S. Department of Energy, Office of Science, Office of Energy, Efficiency, and Renewable Energy, under Award Number DE-SC0023357. This work was also supported by the Delaware Space Grant College and Fellowship Program (NASA Grant 80NSSC20M0045).

VOCABULARY

Membrane permeance	The rate at which a gas species passes through a membrane normalized by the partial pressure difference across the membrane. Permeability is a similar parameter that is also normalized by membrane thickness.
Membrane selectivity	The measure of membrane separation efficiency, defined as the ratio of permeabilities or permeances of the separated gas species.
Zeolite	Porous crystalline aluminosilicate materials with ion-exchangeable cations. The Al/Si ratio and cation species influence the porosity and hydrophobicity.
Ionic liquid (IL)	Compounds of bulky organic cations and organic or inorganic anions characterized by low melting points and remaining liquid at temperatures below 100 °C.
Recycle membrane reactor (RMR)	A reactor and membrane separator configured in series.
Catalytic membrane reactor (CMR)	A reactor and membrane separator configured in parallel, so that reaction and separation occur in one unit.

REFERENCES

(1) Erisman, J. W.; Sutton, M. A.; Galloway, J.; Klimont, Z.; Winiwarter, W. How a Century of Ammonia Synthesis Changed the World. *Nat. Geosci.* **2008**, *1* (10), 636−639.

(2) Padinjarekutt, S.; Li, H.; Ren, S.; Ramesh, P.; Zhou, F.; Li, S.; Belfort, G.; Yu, M. Na^+-Gated Nanochannel Membrane for Highly Selective Ammonia (NH_3) Separation in the Haber-Bosch Process. *Chemical Engineering Journal* **2023**, *454*, No. 139998.

(3) Zhang, Z.; Way, J. D.; Wolden, C. A. Design and Operational Considerations of Catalytic Membrane Reactors for Ammonia Synthesis. *AIChE J.* **2021**, *67* (8), No. e17259.

(4) Sazali, N.; Mohamed, M. A.; Salleh, W. N. W. Membranes for hydrogen separation: A significant review. *International Journal of Advanced Manufacturing Technology* **2020**, *107*, 1859−1881.

(5) Giddey, S.; Badwal, S. P. S.; Munnings, C.; Dolan, M. Ammonia as a Renewable Energy Transportation Media. *ACS Sustain. Chem. Eng.* **2017**, *5*, 10231−10239.

(6) Appl, M., Ammonia. In *Ullmann's Encyclopedia of Industrial Chemistry*; Wiley Online Library, 2000.

(7) Appl, M. *The Haber-Bosch Process and the Development of Chemical Engineering*; Plenum Press: New York, 1982; 29−54.

(8) Bosch, C. Process of Producing Ammonia. US990191A, April 18, 1911.

(9) Ertl, G. Primary Steps in Catalytic Synthesis of Ammonia. *J. Vac. Sci. Technol. A* **1983**, *1* (2), 1247−1253.

(10) Erfani, N.; Baharudin, L.; Watson, M. Recent Advances and Intensifications in Haber-Bosch Ammonia Synthesis Process. *Chemical Engineering and Processing - Process Intensification* **2024**, *204*, No. 109962.

(11) Lin, B.; Wiesner, T.; Malmali, M. Performance of a Small-Scale Haber Process: A Techno-Economic Analysis. *ACS Sustainable Chem. Eng.* **2020**, *8* (41), 15517−15531.

(12) Mersch, M.; Sunny, N.; Dejan, R.; Ku, A. Y.; Wilson, G.; O'Reilly, S.; Soloveichik, G.; Wyatt, J.; Dowell, N. M. A Comparative Techno-Economic Assessment of Blue, Green, and Hybrid Ammonia Production in the United States. *Sustain. Energy Fuels* **2024**, *8* (7), 1495−1508.

(13) Aika, K. I.; Christiansen, L. J.; Dybkjaer, I.; Hansen, J. B.; Nielsen, P. H.; Nielsen, A.; Stoltze, P.; Tamaru, K. *Ammonia: Catalysis and Manufacture*; Springer Science & Business Media, 2012.

(14) Ye, L.; Li, H.; Xie, K. Sustainable Ammonia Production Enabled by Membrane Reactor. *Nat. Sustain.* **2022**, *5* (9), 787−794.

(15) Klinsrisuk, S.; Tao, S.; Irvine, J. T. S. Membrane Reactors for Ammonia Production. In *Membrane Reactors for Energy Applications and Basic Chemical Production*; Elsevier, 2015; 543−563.

(16) Weng, G.; Ouyang, K.; Lin, X.; Xue, J.; Wang, H. Proton Conducting Membranes for Hydrogen and Ammonia Production. *React. Chem. Eng.* **2021**, *6* (10), 1739−1770.

(17) Mansourian, R.; Mousavi, S. M.; Rahimpour, M. R. Membrane Reactors for Ammonia Synthesis/Production. In *Progresses in Ammonia: Science, Technology and Membranes*; Elsevier, 2024; 111−130.

(18) Itoh, M.; Machida, K.; Adachi, G. Ammonia Production Characteristics of Ru/Al_2O_3 Catalysts Using Hydrogen Permeable Membrane. *Chem. Lett.* **2000**, *29* (10), 1162−1163.

(19) Iwahara, H.; Esaka, T.; Uchida, H.; Maeda, N. Proton Conduction in Sintered Oxides and Its Application to Steam Electrolysis for Hydrogen Production. *Solid State Ionics* **1981**, *3*−*4*, 359−363.

(20) Wang, J.-D.; Xie, Y.-H.; Zhang, Z.-F.; Liu, R.-Q.; Li, Z.-J. Protonic Conduction in Ca^{2+}-Doped $La_2M_2O_7$ (M = Ce, Zr) with Its Application to Ammonia Synthesis Electrochemically. *Mater. Res. Bull.* **2005**, *40* (8), 1294−1302.

(21) Xie, Y.-H.; Wang, J.-D.; Liu, R.-Q.; Su, X.-T.; Sun, Z.-P.; Li, Z.-J. Preparation of $La_{1.9}Ca_{0.1}Zr_2O_{6.95}$ with Pyrochlore Structure and Its Application in Synthesis of Ammonia at Atmospheric Pressure. *Solid State Ionics* **2004**, *168* (1), 117−121.

(22) Murakami, T.; Nishikiori, T.; Nohira, T.; Ito, Y. Investigation of Anodic Reaction of Electrolytic Ammonia Synthesis in Molten Salts Under Atmospheric Pressure. *J. Electrochem. Soc.* **2005**, *152* (5), D75.

(23) Haile, S. M.; Boysen, D. A.; Chisholm, C. R. I.; Merle, R. B. Solid Acids as Fuel Cell Electrolytes. *Nature* **2001**, *410* (6831), 910−913.

(24) Richard, S.; Verde, V.; Kezibri, N.; Makhloufi, C.; Saker, A.; Gargiulo, I.; Gallucci, F. Power-to-Ammonia Synthesis Process with Membrane Reactors: Techno- Economic Study. *Int. J. Hydrogen Energy* **2024**, *73*, 462−474.

(25) Kucuk, E.; Hasan Koybasi, H.; Avci, A. K. Beyond Equilibrium Ammonia Synthesis in a Membrane and Heat Exchange Integrated Microreactor: A Modeling Study. *Fuel* **2024**, *357*, No. 129858.

(26) Yan, W.; Moriyama, N.; Nagasawa, H.; Kanezashi, M.; Tsuru, T. Green Ammonia Production via a Catalytic Membrane Reactor: Proof of Concept through Experiments and Simulations. *AIChE J.* **2025**, *71* (8), No. e18863.

(27) Yan, W.-W.; Tsuru, T. Overview: Insight into NH_3 Permselective Membranes and Their Application to a Membrane

https://doi.org/10.1021/acsnano.5c12610
ACS Nano 2025, 19, 39535−39563

Reactor for Efficient Ammonia Production. *Sep. Purif. Technol.* **2025**, *370*, No. 133275.
(28) Wakimoto, K.; Yan, W.-W.; Hattori, M.; Hara, M.; Moriyama, N.; Nagasawa, H.; Kanezashi, M.; Tsuru, T. Green Ammonia Production via Recycle Membrane Reactor: Experiment and Process Simulation. *Chemical Engineering Journal* **2024**, *496*, No. 153754.
(29) Brubaker, D. W.; Kammermeyer, K. Separation of Gases by Plastic Membranes - Permeation Rates and Extent of Separation. *Ind. Eng. Chem.* **1954**, *46* (4), 733−739.
(30) Timashev, S. F.; Vorobiev, A. V.; Kirichenko, V. I.; Popkov, Yu. M.; Volkov, V. I.; Shifrina, R. R.; Lyapunov, A. Ya.; Bondarenko, A. G.; Bobrova, L. P. Specifics of Highly Selective Ammonia Transport through Gas-Separating Membranes Based on Perfluorinated Copolymer in the Form of Hollow Fibers. *J. Membr. Sci.* **1991**, *59* (2), 117−131.
(31) Duan, X.; Kim, D.; Narasimharao, K.; Al-Thabaiti, S.; Tsapatsis, M. High-Performance Ammonia-Selective MFI Nanosheet Membranes. *Chem. Commun.* **2021**, *57* (5), 580−582.
(32) Wei, Q.; Lucero, J. M.; Crawford, J. M.; Way, J. D.; Wolden, C. A.; Carreon, M. A. Ammonia Separation from N_2 and H_2 over LTA Zeolitic Imidazolate Framework Membranes. *J. Membr. Sci.* **2021**, *623*, No. 119078.
(33) Robb, W. L. Thin Silicone Membranes-Their Permeation Properties and Some Applications. *Ann. N.Y. Acad. Sci.* **1968**, *146* (1), 119−137.
(34) Laciak, D. V.; Pez, G. P. Ammonia Separation Using Ion Exchange Polymeric Membranes and Sorbents. US4758250A, July 19, 1988.
(35) Pez, G. P.; Laciak, D. V. Ammonia Separation Using Semipermeable Membranes. US4762535A, August 9, 1988.
(36) Semenova, S. I.; Smirnov, S. I.; Belyakov, V. K.; Karachevtsev, V. G.; Dubyaga, V. P.; Kositskaya, L. G.; Savinov, V. M.; Sokolov, L. B.; Nevsky, L. V.; Kiya-Oglu, N. V.; Bondarenko, A. G. *Method for Recovering Ammonia from Gaseous Mixtures*. SU1063774A1, December 30, 1983.
(37) He, Y.; Cussler, E. L. Ammonia permeabilities of perfluorosulfonic membranes in various ionic forms. *J. Membr. Sci.* **1992**, *68* (1−2), 43−52.
(38) Pez, G. P.; Carlin, R. T.; Laciak, D. V.; Sorensen, J. C. Method for Gas Separation. US4761164A, August 2, 1988.
(39) Adejumo, M.; Oleksy, L.; Liguori, S. Innovative NH_3 separation over immobilized molten salt membrane at high temperatures. *Chemical Engineering Journal* **2024**, *479*, No. 147434.
(40) Camus, O.; Perera, S.; Crittenden, B.; van Delft, Y. C.; Meyer, D. F.; Pex P, P. A. C.; Kumakiri, I.; Miachon, S.; Dalmon, J.-A.; Tennison, S.; Chanaud, P.; Groensmit, E.; Nobel, W. Ceramic Membranes for Ammonia Recovery. *AIChE J.* **2006**, *52* (6), 2055−2065.
(41) Kanezashi, M.; Yamamoto, A.; Yoshioka, T.; Tsuru, T. Characteristics of Ammonia Permeation through Porous Silica Membranes. *AIChE J.* **2010**, *56* (5), 1204−1212.
(42) Inami, H.; Abe, C.; Hasegawa, Y. Development of Ammonia Selectively Permeable Zeolite Membrane for Sensor in Sewer System. *Membranes* **2021**, *11* (5), 348.
(43) Tanaka, M.; Matsuo, T.; Aoshima, T. Ammonia Separation Method and Zeolite. US10946333B2, March 16, 2021.
(44) Hwan Park, S.; Sengupta, B.; Emami Gerami, S.; Friedman, K.; Lecaros, R.; Ibrahim, M. A. F.; Yu, M. Organic-Free Synthesis of Silicoaluminophosphate Zeotype Membranes with Tunable Framework Charge Density. *J. Mater. Chem. A* **2025**, *13* (6), 4292−4298.
(45) Petukhov, D. I. MXene-Based Gas Separation Membranes with Sorption Type Selectivity. *J. Membr. Sci.* **2021**, *621*, No. 118994.
(46) Jiang, H.; Bai, L.; Wang, Z.; Zheng, W.; Yang, B.; Zeng, S.; Zhang, X.; Zhang, X. Mixed Matrix Membranes Containing Cu-Based Metal Organic Framework and Functionalized Ionic Liquid for Efficient NH_3 Separation. *J. Membr. Sci.* **2022**, *659*, No. 120780.
(47) Liu, L.; Liu, D.; Zhang, C. High-Temperature Hydrogen/Propane Separations in Asymmetric Carbon Molecular Sieve Hollow Fiber Membranes. *J. Membr. Sci.* **2022**, *642*, No. 119978.
(48) Li, J.-R.; Kuppler, R. J.; Zhou, H.-C. Selective Gas Adsorption and Separation in Metal−Organic Frameworks. *Chem. Soc. Rev.* **2009**, *38* (5), 1477−1504.
(49) Hunter, E. P. L.; Lias, S. G. Evaluated Gas Phase Basicities and Proton Affinities of Molecules: An Update. *J. Phys. Chem. Ref. Data* **1998**, *27* (3), 413−656.
(50) Bhown, A.; Cussler, E. L. Mechanism for Selective Ammonia Transport through Poly(Vinylammonium Thiocyanate) Membranes. *J. Am. Chem. Soc.* **1991**, *113* (3), 742−749.
(51) Laciak, D. V.; Pez, G. P.; Burban, P. M. Molten Salt Facilitated Transport Membranes. Part 2. Separation of Ammonia from Nitrogen and Hydrogen at High Temperatures. *J. Membr. Sci.* **1992**, *65*, 31−38.
(52) Adejumo, M.; Fazio, N.; Liguori, S. NH_3 Separation by $ZnCl_2$ Immobilized Molten Salt (IMS): Experimental and Modeling. *J. Membr. Sci.* **2025**, *726*, No. 124053.
(53) Jiang, H.; Bai, L.; Peng, K.; Yuan, L.; Zheng, S.; Zeng, S.; Luo, S.; Zhang, X. Blended Membranes with Ionic Liquids

(69) Yan, W.-W.; Wakimoto, K.; Moriyama, N.; Nagasawa, H.; Kanezashi, M.; Tsuru, T. Development of Sulfonated (3-Mercaptopropyl)Trimethoxysilane Membranes with Thermal Stability and Excellent NH_3 Perm-Selectivity at 300 °C. *J. Membr. Sci.* **2024**, *696*, No. 122535.
(70) Yan, W.-W.; Wakimoto, K.; Moriyama, N.; Nagasawa, H.; Kanezashi, M.; Tsuru, T. Fabrication of 3-(Trihydroxysilyl)-1-Propanesulfonic Acid Membranes with Superior Affinity and Selectivity for NH_3 Permeation over H_2 and N_2 at 50−300 °C. *J. Membr. Sci.* **2024**, *702*, No. 122798.
(71) Vorotyntsev, I. V.; Drozdov, P. N.; Karyakin, N. V. Ammonia permeability of a cellulose acetate membrane. *Inorg. Mater.* **2006**, *42* (3), 231−235.
(72) Browall, W. R. Ultrathin Polyetherimide Membrane and Gas Separation Process. US4156597A, May 29, 1979.
(73) Henis, J. M. S.; Tripodi, M. K. Multicomponent Membranes for Gas Separations. US4230463A, October 28, 1980.
(74) Riley, R. L.; Grabowsky, R. L. Preparation of Gas Separation Membranes. US4243701A, January 6, 1981.
(75) Kulprathipanja, S.; Kulkarni, S. S. Separation of Polar Gases from Nonpolar Gases. US4608060A, August 26, 1986.
(76) Pan, C. Y.; Hadfield, E. M. Permeation Process for Separating Ammonia from a Gas Mixture. US4793829A, December 27, 1988.
(77) Vorotyntsev, I. V.; Shablykin, D. N.; Drozdov, P. N.; Trubyanov, M. M.; Petukhov, A. N.; Battalov, S. V. Separation of Ammonia-Containing Gas Mixtures in a One-Compressor Multistage Membrane Apparatus. *Pet. Chem.* **2017**, *57* (2), 172−181.
(78) Yang, B.; Bai, L.; Wang, Z.; Jiang, H.; Zeng, S.; Zhang, X.; Zhang, X. Exploring NH_3 Transport Properties by Tailoring Ionic Liquids in Pebax-Based Hybrid Membranes. *Ind. Eng. Chem. Res.* **2021**, *60* (26), 9570−9577.
(79) Bikson, B.; Nelson, J. K.; Perrin, J. E. Process for Recovery of Ammonia from an Ammonia-Containing Gas Mixture. US5009678A, April 23, 1991.
(80) Tricoli, V.; Cussler, E. L. Ammonia Selective Hollow Fibers. *J. Membr. Sci.* **1995**, *104* (1), 19−26.
(81) Ansaloni, L.; Dai, Z.; Ryan, J. J.; Mineart, K. P.; Yu, Q.; Saud, K. T.; Hägg, M.-B.; Spontak, R. J.; Deng, L. Solvent-Templated Block Ionomers for Base- and Acid-Gas Separations: Effect of Humidity on Ammonia and Carbon Dioxide Permeation. *Adv. Mater. Interfaces* **2017**, *4* (22), No. 1700854.
(82) Signorini, V.; Askin, A.; Oldani, C.; Minelli, M.; Giacinti Baschetti, M. Study on Ammonia Transport and Separation in Aquivion® Perfluoro Sulfonated Acid Membranes. *J. Membr. Sci.* **2024**, *697*, No. 122564.
(83) Akhmetshina, A. A.; Davletbaeva, I. M.; Grebenschikova, E. S.; Sazanova, T. S.; Petukhov, A. N.; Atlaskin, A. A.; Razov, E. N.; Zaripov, I. I.; Martins, C. F.; Neves, L. A.; Vorotyntsev, I. V. The Effect of Microporous Polymeric Support Modification on Surface and Gas Transport Properties of Supported Ionic Liquid Membranes. *Membranes* **2016**, *6* (1), 4.
(84) Yang, B.; Bai, L.; Zeng, S.; Luo, S.; Liu, L.; Han, J.; Nie, Y.; Zhang, X.; Zhang, S. NH_3 Separation Membranes with Self-Assembled Gas Highways Induced by Protic Ionic Liquids. *Chemical Engineering Journal* **2021**, *421*, No. 127876.
(85) Shukla, S. K. A Fixed-Site Carrier Composite Membrane for NH_3/N_2 Separation. *Gas Sep. Purif.* **1992**, *6* (2), 79−81.
(86) Jiang, H.; Yang, B.; Peng, K.; Liu, Z.; Zeng, S.; Zhang, X.; Bai, L. Metal Ionic Liquid-Based Hybrid Membranes for Ammonia Separation through Moderate Interaction Sites and Cooperative Transport Channels. *Chem. Eng. Sci.* **2024**, *299*, No. 120464.
(87) Zheng, W.; Liu, Z.; Deng, J.; Dong, H.; Bai, L.; Zhang, X. Ammonia-Philic Ionic Liquids Decorated Nanochannels of Two-Dimensional LDH Membranes for Selective NH_3 Separation. *Sep. Purif. Technol.* **2025**, *358*, No. 130282.
(88) Stepan, O.; Stverak, B. *Influence of Ionizing Radiation on the Catalytic Activity of Iron Catalysts for Ammonia Synthesis*; Inst. for Research, Production, and Use of Radioisotopes: Prague, **1971**.
(89) Almquist, J.; Crittenden, E. A Study of Pure-Iron and Promoted-Iron Catalysts for Ammonia Synthesis. *J. Industrial Engineering Chemistry* **1926**, *18* (12), 1307−1309.
(90) Aika, K.-I.; Ozaki, A. Kinetics and Isotope Effect of Ammonia Synthesis Over a Singly-Promoted Iron Catalyst. *J. Catal.* **1970**, *19* (3), 350−352.
(91) Dumesic, J.; Topsøe, H.; Khammouma, S.; Boudart, M. Surface, Catalytic and Magnetic Properties of Small Iron Particles: II. Structure Sensitivity of Ammonia Synthesis. *J. Catal.* **1975**, *37* (3), 503−512.
(92) Van Ommen, J.; Bolink, W.; Prasad, J.; Mars, P. The Nature of the Potassium Compound Acting as a Promoter in Iron-Alumina Catalysts for Ammonia Synthesis. *J. Catal.* **1975**, *38* (1−3), 120−127.
(93) Altenburg, K.; Bosch, H.; Van Ommen, J.; Gellings, P. The Role of Potassium as a Promoter in Iron Catalysts for Ammonia Synthesis. *J. Catal.* **1980**, *66* (2), 326−334.
(94) Xiujin, Y.; Bingyu, L.; Jianxin, L.; Rong, W.; Kemei, W. A Novel Fused Iron Catalyst for Ammonia Synthesis Promoted with Rare Earth Gangue. *J. Rare Earths* **2008**, *26* (5), 711−716.
(95) Wang, P.; Chang, F.; Gao, W.; Guo, J.; Wu, G.; He, T.; Chen, P. Breaking Scaling Relations to Achieve Low-Temperature Ammonia Synthesis Through LiH-Mediated Nitrogen Transfer and Hydrogenation. *Nat. Chem.* **2017**, *9* (1), 64−70.
(96) Gao, W.; Guo, J.; Wang, P.; Wang, Q.; Chang, F.; Pei, Q.; Zhang, W.; Liu, L.; Chen, P. Production of Ammonia via a Chemical Looping Process Based on Metal Imides as Nitrogen Carriers. *Nature Energy* **2018**, *3* (12), 1067−1075.
(97) Humphreys, J.; Lan, R.; Du, D.; Xu, W. Promotion Effect of Proton-Conducting Oxide BaZr0.1Ce0. 7Y0. 2O3− on the Catalytic Activity of Ni Towards Ammonia Synthesis from Hydrogen and Nitrogen. *Int. J. Hydrogen Energy* **2018**, *43* (37), 17726−17736.
(98) Tang, Y.; Kobayashi, Y.; Masuda, N.; Uchida, Y.; Okamoto, H.; Kageyama, T.; Hosokawa, S.; Loyer, F.; Mitsuhara, K.; Yamanaka, K. Metal-Dependent Support Effects of Oxyhydride-Supported Ru, Fe, Co Catalysts for Ammonia Synthesis. *Adv. Energy Mater.* **2018**, *8* (36), No. 1801772.
(99) Kitano, M.; Kujirai, J.; Ogasawara, K.; Matsuishi, S.; Tada, T.; Abe, H.; Niwa, Y.; Hosono, H. Low-Temperature Synthesis of Perovskite Oxynitride-Hydrides as Ammonia Synthesis Catalysts. *J. Am. Chem. Soc.* **2019**, *141* (51), 20344−20353.
(100) Wang, Z.; Lin, J.; Wang, R.; Wei, K. Ammonia Synthesis Over Ruthenium Catalyst Supported on Perovskite Type $BaTiO_3$. *Catal. Commun.* **2013**, *32*, 11−14.
(101) Bielawa, H.; Hinrichsen, O.; Birkner, A.; Muhler, M. The Ammonia-Synthesis Catalyst of the Next Generation: Barium-Promoted Oxide-Supported Ruthenium. *Angew. Chem., Int. Ed.* **2001**, *40* (6), 1061−1063.
(102) Honkala, K.; Hellman, A.; Remediakis, I.; Logadottir, A.; Carlsson, A.; Dahl, S.; Christensen, C. H.; Nørskov, J. K. Ammonia Synthesis From First-Principles Calculations. *Science* **2005**, *307* (5709), 555−558.
(103) García-García, F. R.; Guerrero-Ruiz, A.; Rodríguez-Ramos, I. Role of B_5-Type Sites in Ru Catalysts Used for the NH_3 Decomposition Reaction. *Top. Catal.* **2009**, *52* (6), 758−764.
(104) Jacobsen, C. J.; Dahl, S.; Hansen, P. L.; Törnqvist, E.; Jensen, L.; Topsøe, H.; Prip, D. V.; Møenshaug, P. B.; Chorkendorff, I. Structure Sensitivity of Supported Ruthenium Catalysts for Ammonia Synthesis. *J. Mol. Catal. A: Chem.* **2000**, *163* (1−2), 19−26.
(105) Narasimharao, K.; Seetharamulu, P.; Rao, K. R.; Basahel, S. N. Carbon Covered Mg−Al Hydrotalcite Supported Nanosized Ru Catalysts for Ammonia Synthesis. *J. Mol. Catal. A: Chem.* **2016**, *411*, 157−166.
(106) Li, J.; Wang, W.; Chen, W.; Gong, Q.; Luo, J.; Lin, R.; Xin, H.; Zhang, H.; Wang, D.; Peng, Q. Sub-nm Ruthenium Cluster as an Efficient and Robust Catalyst for Decomposition and Synthesis of Ammonia: Break the "Size Shackles". *Nano Res.* **2018**, *11*, 4774−4785.
(107) Ogura, Y.; Sato, K.; Miyahara, S.-i; Kawano, Y.; Toriyama, T.; Yamamoto, T.; Matsumura, S.; Hosokawa, S.; Nagaoka, K. Efficient

https://doi.org/10.1021/acsnano.5c12610
ACS Nano 2025, 19, 39535−39563

Ammonia Synthesis Over a Ru/$La_{0.5}Ce_{0.5}O_{1.75}$ Catalyst Pre-Reduced at High Temperature. *Chemical Science* **2018**, *9* (8), 2230−2237.
(108) Inoue, Y.; Kitano, M.; Kim, S.-W.; Yokoyama, T.; Hara, M.; Hosono, H. Highly dispersed Ru on Electride $[Ca_{24}Al_{28}O_{64}]^{4+}(e-)_4$ as a Catalyst for Ammonia Synthesis. *ACS Catal.* **2014**, *4* (2), 674−680.
(109) Kobayashi, Y.; Tang, Y.; Kageyama, T.; Yamashita, H.; Masuda, N.; Hosokawa, S.; Kageyama, H. Titanium-Based Hydrides as Heterogeneous Catalysts for Ammonia Synthesis. *J. Am. Chem. Soc.* **2017**, *139* (50), 18240−18246.
(110) Hattori, M.; Mori, T.; Arai, T.; Inoue, Y.; Sasase, M.; Tada, T.; Kitano, M.; Yokoyama, T.; Hara, M.; Hosono, H. Enhanced Catalytic Ammonia Synthesis with Transformed BaO. *ACS Catal.* **2018**, *8* (12), 10977−10984.
(111) Lin, B.; Guo, Y.; Cao, C.; Ni, J.; Lin, J.; Jiang, L. Carbon Support Surface Effects in the Catalytic Performance of Ba-Promoted Ru Catalyst for Ammonia Synthesis. *Catal. Today* **2018**, *316*, 230−236.
(112) Kitano, M.; Inoue, Y.; Sasase, M.; Kishida, K.; Kobayashi, Y.; Nishiyama, K.; Tada, T.; Kawamura, S.; Yokoyama, T.; Hara, M. Self-organized Ruthenium−Barium Core−Shell Nanoparticles on a Mesoporous Calcium Amide Matrix for Efficient Low-Temperature Ammonia Synthesis. *Angew. Chem., Int. Ed.* **2018**, *57* (10), 2648−2652.
(113) Hattori, M.; Iijima, S.; Nakao, T.; Hosono, H.; Hara, M. Solid Solution for Catalytic Ammonia Synthesis from Nitrogen and Hydrogen Gases at 50 °C. *Nat. Commun.* **2020**, *11* (1), 2001.
(114) Wildfire, C.; Abdelsayed, V.; Shekhawat, D.; Dagle, R. A.; Davidson, S. D.; Hu, J. Microwave-Assisted Ammonia Synthesis Over Ru/MgO Catalysts at Ambient Pressure. *Catal. Today* **2021**, *365*, 103−110.
(115) Humphreys, J.; Lan, R.; Tao, S. Development and Recent Progress on Ammonia Synthesis Catalysts for Haber−Bosch Process. *Adv. Energy Sustain. Res.* **2021**, *2* (1), No. 2000043.
(116) Wang, X.; Li, L.; Fang, Z.; Zhang, Y.; Ni, J.; Lin, B.; Zheng, L.; Au, C.-t.; Jiang, L. Atomically Dispersed Ru Catalyst for Low-Temperature Nitrogen Activation to Ammonia via an Associative Mechanism. *ACS Catal.* **2020**, *10* (16), 9504−9514.
(117) Rosowski, F.; Hornung, A.; Hinrichsen, O.; Herein, D.; Muhler, M.; Ertl, G. Ruthenium Catalysts for Ammonia Synthesis at High Pressures: Preparation, Characterization, and Power-Law Kinetics. *Applied Catalysis A: General* **1997**, *151* (2), 443−460.
(118) Hagen, S.; Barfod, R.; Fehrmann, R.; Jacobsen, C. J.; Teunissen, H. T.; Ståhl, K.; Chorkendorff, I. New Efficient Catalyst for Ammonia Synthesis: Barium-Promoted Cobalt on Carbon. *Chem. Commun.* **2002**, *11*, 1206−1207.
(119) Raróg-Pilecka, W.; Miśkiewicz, E.; Matyszek, M.; Kaszkur, Z.; Kępiński, L.; Kowalczyk, Z. Carbon-Supported Cobalt Catalyst for Ammonia Synthesis: Effect of Preparation Procedure. *J. Catal.* **2006**, *237* (1), 207−210.
(120) Raróg-Pilecka, W.; Miśkiewicz, E.; Kępiński, L.; Kaszkur, Z.; Kielar, K.; Kowalczyk, Z. Ammonia Synthesis Over Barium-promoted Cobalt Catalysts Supported on Graphitised Carbon. *J. Catal.* **2007**, *249* (1), 24−33.
(121) Raróg-Pilecka, W.; Miśkiewicz, E.; Kowalczyk, Z. Activated Carbon as a Template for Creating Catalyst Precursors. Unsupported Cobalt Catalyst for Ammonia Synthesis. *Catal. Commun.* **2008**, *9* (5), 870−873.
(122) Raróg-Pilecka, W.; Karolewska, M.; Truszkiewicz, E.; Iwanek, E.; Mierzwa, B. Cobalt Catalyst Doped with Cerium and Barium Obtained by Co-Precipitation Method for Ammonia Synthesis Process. *Catal. Lett.* **2011**, *141*, 678−684.
(123) Lin, B.; Qi, Y.; Wei, K.; Lin, J. Effect of Pretreatment on Ceria-Supported Cobalt Catalyst for Ammonia Synthesis. *RSC Adv.* **2014**, *4* (72), 38093−38102.
(124) Tarka, A.; Zybert, M.; Truszkiewicz, E.; Mierzwa, B.; Kępiński, L.; Moszyński, D.; Raróg-Pilecka, W. Effect of a Barium Promoter on the Stability and Activity of Carbon-Supported Cobalt Catalysts for Ammonia Synthesis. *ChemCatChem.* **2015**, *7* (18), 2836−2839.
(125) Han, A.; Wang, B.; Kumar, A.; Qin, Y.; Jin, J.; Wang, X.; Yang, C.; Dong, B.; Jia, Y.; Liu, J. Recent Advances for MOF-Derived Carbon-Supported Single-Atom Catalysts. *Small Methods* **2019**, *3* (9), No. 1800471.
(126) Wang, X.; Peng, X.; Chen, W.; Liu, G.; Zheng, A.; Zheng, L.; Ni, J.; Au, C.-t.; Jiang, L. Insight into Dynamic and Steady-State Active Sites for Nitrogen Activation to Ammonia by Cobalt-Based Catalyst. *Nat. Commun.* **2020**, *11* (1), 653.
(127) Zhou, Y.; Wang, C.; Peng, X.; Zhang, T.; Wang, X.; Jiang, Y.; Qi, H.; Zheng, L.; Lin, J.; Jiang, L. Boosting Efficient Ammonia Synthesis Over Atomically Dispersed Co-Based Catalyst via the Modulation of Geometric and Electronic Structures. *CCS Chemistry* **2022**, *4* (5), 1758−1769.
(128) Li, X.; Jiao, Y.; Cui, Y.; Dai, C.; Ren, P.; Song, C.; Ma, X. Interfaces, Synergistic Catalysis of the Synthesis of Ammonia with Co-Based Catalysts and Plasma: From Nanoparticles to a Single Atom. *ACS Applied Materials* **2021**, *13* (44), 52498−52507.
(129) Peng, X.; Cai, H.; Zhou, Y.; Ni, J.; Wang, X.; Lin, B.; Lin, J.; Zheng, L.; Au, C.-t; Jiang, L. Studies of a Highly Active Cobalt Atomic Cluster Catalyst for Ammonia Synthesis. *ACS Sustainable Chemistry Engineering* **2022**, *10* (5), 1951−1960.
(130) Hargreaves, J. Heterogeneous Catalysis with Metal Nitrides. *Coord. Chem. Rev.* **2013**, *257* (13−14), 2015−2031.
(131) Jacobsen, C. J.; Dahl, S.; Clausen, B. S.; Bahn, S.; Logadottir, A.; Nørskov, J. K. Catalyst Design by Interpolation in the Periodic Table: Bimetallic Ammonia Synthesis Catalysts. *J. Am. Chem. Soc.* **2001**, *123* (34), 8404−8405.
(132) Jacobsen, C. J. Novel Class of Ammonia Synthesis Catalysts. *Chem. Commun.* **2000**, *12*, 1057−1058.
(133) Kojima, R.; Aika, K.-i Cobalt Molybdenum Bimetallic Nitride Catalysts for Ammonia Synthesis: Part 1. Preparation and Characterization. *Applied Catalysis A: General* **2001**, *215* (1−2), 149−160.
(134) Azofra, L. M.; Morlanés, N.; Poater, A.; Samantaray, M. K.; Vidjayacoumar, B.; Albahily, K.; Cavallo, L.; Basset, J. M. Single-Site Molybdenum on Solid Support Materials for Catalytic Hydrogenation of N_2-into-NH_3. *Angew. Chem., Int. Ed.* **2018**, *57* (48), 15812−15816.
(135) Cao, H.; Guo, J.; Chang, F.; Pistidda, C.; Zhou, W.; Zhang, X.; Santoru, A.; Wu, H.; Schell, N.; Niewa, R. Transition and Alkali Metal Complex Ternary Amides for Ammonia Synthesis and Decomposition. *Chem.−Eur. J.* **2017**, *23* (41), 9766−9771.
(136) Ye, T.-N.; Park, S.-W.; Lu, Y.; Li, J.; Sasase, M.; Kitano, M.; Tada, T.; Hosono, H. Vacancy-Enabled N_2 Activation for Ammonia Synthesis on an Ni-Loaded Catalyst. *Nature* **2020**, *583* (7816), 391−395.
(137) Ye, T.-N.; Park, S.-W.; Lu, Y.; Li, J.; Sasase, M.; Kitano, M.; Hosono, H. Contribution of Nitrogen Vacancies to Ammonia Synthesis Over Metal Nitride Catalysts. *J. Am. Chem. Soc.* **2020**, *142* (33), 14374−14383.
(138) Li, Z.; Lu, Y.; Li, J.; Xu, M.; Qi, Y.; Park, S.-W.; Kitano, M.; Hosono, H.; Chen, J.-S.; Ye, T.-N. Multiple Reaction Pathway on Alkaline Earth Imide Supported Catalysts for Efficient Ammonia Synthesis. *Nat. Commun.* **2023**, *14* (1), 6373.
(139) Li, W. Q.; Xu, M.; Chen, J. S.; Ye, T. N. Enabling Sustainable Ammonia Synthesis: From Nitrogen Activation Strategies to Emerging Materials. *Adv. Mater.* **2024**, *36* (40), No. 2408434.
(140) Lu, X.; Wu, J.; He, X.; Li, Z.; Lu, Y.; Li, W.; Li, J.; Xu, M.; Qi, Y.; Zhang, Q.; Liu, Y.; Du, M.; Kamiya, T.; Hosono, H.; Pan, F.; Chen, J.; Ye, T. N. Ordered Single Active Sites for Cascade Hydrogenation and Hydroformylation Reactions. *Nat. Catal.* **2025**, *8*, 536−547.
(141) Mallick, A.; Mayorga-Martinez, C. C.; Pumera, M. Low-dimensional Materials for Ammonia Synthesis. *Chem. Soc. Rev.* **2025**, *54*, 5021.
(142) Zheng, L.; Ambrosetti, M.; Tronconi, E. Joule-Heated Catalytic Reactors toward Decarbonization and Process Intensification: A Review. *ACS Eng. Au* **2024**, *4* (1), 4−21.
(143) Gorky, F.; Nguyen, H. M.; Lucero, J. M.; Guthrie, S.; Crawford, J. M.; Carreon, M. A.; Carreon, M. L. CC3 Porous Organic Cage Crystals and Membranes for the Non-Thermal Plasma Catalytic

https://doi.org/10.1021/acsnano.5c12610
ACS Nano 2025, 19, 39535−39563

Ammonia Synthesis. *Chemical Engineering Journal Advances* **2022**, *11*, No. 100340.
(144) Dong, Q.; Yao, Y.; Cheng, S.; Alexopoulos, K.; Gao, J.; Srinivas, S.; Wang, Y.; Pei, Y.; Zheng, C.; Brozena, A. H.; Zhao, H.; Wang, X.; Toraman, H. E.; Yang, B.; Kevrekidis, I. G.; Ju, Y.; Vlachos, D. G.; Liu, D.; Hu, L. Programmable Heating and Quenching for Efficient Thermochemical Synthesis. *Nature* **2022**, *605* (7910), 470–476.

https://doi.org/10.1021/acsnano.5c12610
ACS Nano 2025, 19, 39535–39563